The study of temperature and night green airglow at mid-latitude in MLT during winter

Zorkaltseva, O., Vasilyev, R., Saunkin, A., Pogoreltsev, A.

O. S. Zorkaltseva, R. V. Vasilyev, A. V. Saunkin, A. I. Pogoreltsev, "The study of temperature and night green airglow at mid-latitude in MLT during winter," Proc. SPIE 11560, 26th International Symposium on Atmospheric and Ocean Optics, Atmospheric Physics, 1156081 (12 November 2020); doi: 10.1117/12.2574914

SPIE.

Event: 26th International Symposium on Atmospheric and Ocean Optics, Atmospheric Physics, 2020, Moscow, Russian Federation

The study of temperature and night green airglow at mid-latitude in MLT during winter

Zorkaltseva O.S.[1,2], Vasilyev R.V.[1,2], Saunkin A.V. [1], Pogoreltsev A.I. [3]
[1]Institute of Solar-Terrestrial Physics SB RAS, Irkutsk, Russia
[2]Irkutsk State University, Irkutsk, Russia
[3]Russian Hydrometeorological University, Saint-Petersburg, Russia.

ABSTRACT

We studied the temperature and the emission of 557.7 nm in the MLT in the geophysical observatory "Tory" (51.8N, 103.1E) during winter 2018-2019. For analysis, we used the measurement data of the Fabry-Perot interferometer (FPI), the SABER/TIMED data, the data of the model of middle and upper atmosphere (MUAM) and the data of the ERA-interim archive. It turned out that MLT emission is decreases during an increase in the amplitude of a stationary planetary wave with a zonal wave number 1 in the stratosphere, as well as during sudden stratospheric warmings. However, the temperature according to the FPI data increases, and according to the SABER data temperature decreases during these events in the stratosphere. In this paper we discuss the reasons for these differences, which are caused by a variation in the height of the emission layer and by the features of the SABER observations. The MUAM data confirm our assumptions about the reasons for the differences between SABER and FPI temperature.
Keywords: MLT temperature, emission 557.7nm, sudden stratospheric warming, planetary wave.

1. INTRODUCTION

The study of the upper atmosphere is relevant for the fundamental problems of atmospheric physics and for practical purposes. First, it is necessary to understand the long-term trends in the composition and dynamic characteristics of the upper layers, as well as a deeper understanding of the mechanisms of vertical interaction between atmospheric layers. Based on this knowledge, it would be possible to create models of the Earth system and predict the parameters of the upper atmosphere, which would be useful, for example, for the exploitation of low-orbit satellites. However, regular monitoring of the upper atmosphere requires complex and expensive instruments, therefore, the observation of MLT is carried out in separate observatories that are not combined into a global system. The successes of ground-based monitoring of MLT have observations on meteor radars. According to meteor radar data, the climatology of wind speed, tides, latitudinal and longitudinal dependence of wind and the reaction to sudden stratospheric warming were studied. [1,2,3,4,5]. MLT temperature is usually obtained from lidar data (below 80 km), interferometric [6,7] and spectrometric [8,9] observations of atmospheric airglow. Satellites are also an important source of MLT temperature. Satellite instruments provide a global picture, but have a limited local time sample, and many also have limited spatial resolution [10]. Southern Siberia, where we are observing, is one of the region that is not covered by measurements of the upper atmosphere. Earlier (1976–1996), in Eastern Siberia, the wind of MLT was monitored by method to receive signals from the separated radio reception of broadcasting stations in the long wavelength range [11].

The monitoring of temperature regime in Siberia region provided by the hydroxyl emission spectral observations at geophysical station (Tory) Institute of Solar-Terrestrial Physics [12, 13]. It turned out, that the MLT heights a significant increase in the OH and O2 emission intensities, a decrease in the atmosphere temperature, and an increase in wave

26th International Symposium on Atmospheric and Ocean Optics, Atmospheric Physics, edited by Gennadii G. Matvienko, Oleg A. Romanovskii, Proc. of SPIE Vol. 11560, 1156081
© 2020 SPIE · CCC code: 0277-786X/20/$21 · doi: 10.1117/12.2574914

activity were observed during SSW. It turned out, that a significant increase in the OH and O2 emission intensities, a decrease in the atmosphere temperature at the MLT, and an increase in wave activity were observed during SSW. The results of works [12, 13] are confirmed by satellite data. Our observations on the Fabry-Perot interferometer contradict the conclusions that the temperature in MLT decreases during CER and we will consider the reasons for the inconsistency of the MLT reaction to the stratospheric effect.

2. DATA AND METHODS

In this paper, we use FPI data on the behavior of the temperature. An FPI with a temporal resolution of about 10–15 minutes observes the upper atmosphere parameters using emission lines of atomic oxygen 557.7 nm. The heights of this emission are about 95 km. The wind speed and the air temperature over the observation place was restored using emission line doppler shifting and doppler broadening due to the movement of excited atomic oxygen O(1S). More details about FPI are described in the paper [7, 14, 15].

We compared the FPI data with Sounding of the Atmosphere using Broadband Emission Radiometry (SABER) which is one of four instruments on the NASA TIMED satellite (Thermosphere Ionosphere Mesosphere Energetics and Dynamics). The main goal of SABER is to provide data on the fundamental processes that regulate energy, chemistry, dynamics and transport in the mesosphere and lower thermosphere. SABER accomplishes this with global atmospheric measurements using a 10-channel broadband infrared radiometer using a limb scan method covering the spectral range from 1.27 to 17 microns. These measurements are used to obtain vertical profiles of kinetic temperature, pressure, geopotential height, volumetric ratios for trace elements O3, CO2, H2O, [O] and [H], volumetric emissions for 5.3 μm NO, 2.1 μm OH, 1.6 μm OH and 1.27 μm O2 (1Δ), cooling and heating rates for many bands of CO2, O3 and O2, as well as chemical heating rates for 7 important reactions [http://saber.gats-inc.com/overview.php].

To calculate the concentration of atomic oxygen using SABER data, we apply the method described in [16]. The main idea there was to use the mesospheric ozone balance in nighttime. The hydroxyl emission was used as marker of mesospheric ozone loss in the reaction with the hydrogen and the balanced ozone production in this case appeared due to reaction of recombination in triple collision of atomic and molecular oxygen with any other spice of atmosphere. Taking in to account all the quenching factors for hydroxyl optical emission and measured by SABER the air temperature, air density and ozone mixing ratio one can solve the quadratic equation to get the atomic oxygen concentration.

If we know the atomic oxygen concentration, we can calculate volume emission rate for 558 mn oxygen line (VER558) using inversion of method of atomic oxygen concentration extraction from [Gao et al. 16]. Here is supposed that the production of excited O(1S) governed by the Barth mechanism in triple collision of two oxygen atoms with any other atmosphere spice. All the other needed inputs for the VER558 formulae (1) in [17] we also got from SABER data.

Result of the VER558 height profile calculation is shown in fig 1 where we present averaged over period of two year VER558 height profiles obtained using SABER data height profiles in the spatial area about 1400 km in diameter over the FPI. As one can see the height of maximum VER558 is placed near 95 km height and placed slightly below the temperature minimum. To make a correct comparison the themperatures measured by FPI and SABER we select the measurements made by both instruments near the same time in described area over FPI and average the SABER temperature profile in range 90-100 km using VER558 values as a weights and normalizing the result by integral of VER558 in the same height range.

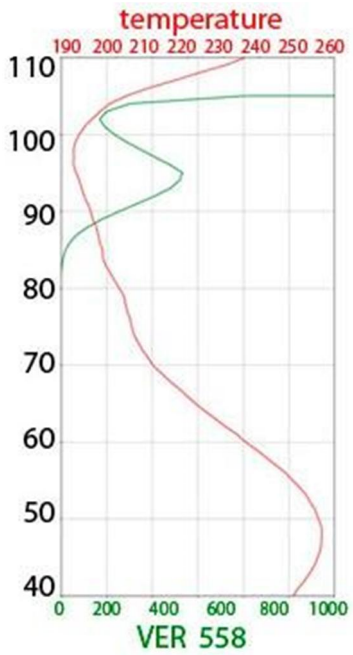

Figure 1 The averaged vertical profile of 557.7 nm emission (green) and vertical profile of the temperature (red) obtained user SABER data and methods described.

To study the characteristics of the SSW, the climate archive of the ECMWF Era-interim was used. In accordance with the SSW criteria established by the WMO, parameters such as the zonal average air temperature along 80N and zonal average values of the zonal component of the wind along 60N at the height 10 hPa on a grid of 2.5x2.5 degrees were considered. The amplitudes of stationary planetary waves along a 60N with zonal wave numbers 1 and 2 were also considered (SPW1 and SPW2, respectively).

3. RESULTS

Fig. 2 shows the daily zonal mean zonal wind at 60N (blue) and the temperature at 80N (red) obtained from the ERA-Interim reanalysis dataset for the period from 1 October 2018 to 31 March 2019, observed at 10 hPa (solid) and at 1 hPa (dotted). During the winter, we see that two stratospheric warmings were observed with a peak on Feb 1 (251 K) and Feb 27 (251 K), SSW1 and SSW2 respectively, marked by dotted vertical lines in the figure. The grey rectangles show duration of SSW. As a criterion for the onset of warming, we took a day with a sharp increase in temperature (more than 10 degrees per day). We thought the end of the SSW was when the temperature sharp decrease of temperature ended (about 2 degrees).

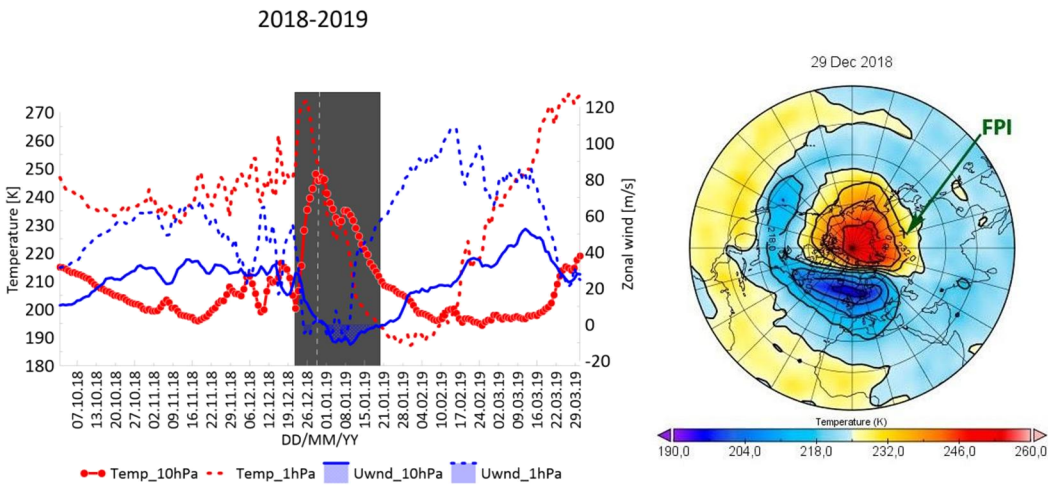

Figure 2: Left - daily zonal mean of the zonal wind at 10 hPa (blue solid line), at 1 hPa (blue dotted line) and zonal mean temperature at 10 hPa (red solid line) and at 1 hPa (red dotted line) obtained from ERA-Interim reanalysis dataset from 1 Oct 2018 to 31 Mar 2019. Right - distribution of temperature at 10 hPa in stereographic projection on maximum SSW. Green arrow show location of the FPI.

In the winter season 2018-2019, one SSW was observed. SSW arose on Dec 22 and lasted until January 19. The maximum temperature at this warming was 248K on Dec 29 (Fig 4 right). An increase in temperature was observed throughout the stratosphere. During warming, the wind changed direction to the westward. FPI was in the area of warming this winter (Fig 2 left).

In Figure 3, we noted the periods of SSW (gray rectangle), the day of maximum SSW temperature (dotted white vertical line), and periods increased activity of planetary waves (light gray rectangle). The amplitudes of stationary planetary waves were calculated along 60N with zonal wave numbers 1 and 2 (SPW1 and SPW2, respectively) according to Era-interim data. Figure 3 show a FPI & SABER 557.7nm emission decrease during increase SSW. We can also see that a decrease in intensity is observed at moments without stratospheric warming. However, we note that low emission is always observed during increased activity of planetary waves, especially SPW1. Tory FPI temperature and SABER temperature have more reasonable values, but the behavior of the temperature during the SSW and SPW is opposite (Figure 4). The temperature observed by FPI is increased, while temperature observed by SABER is decreased. The difference can be explained by the different heights of the radiation formation. The green line can be radiated from the heights with more high temperature and reach values up to 250 K as the height gradient of the temperature over the mesopause can be extremely high (up to 10K/km). The increasing of the temperature with the decreasing of 557.7 emission can also be explained discussed above increasing of the 557.7 layer emission height. In this case the increasing of surrounding temperature will lead to decreasing of 557.7 nm line intensity due to decreasing of precursor of O(1S) state (excited O2) forming in the Barth mechanism with rate inversely depending on the temperature. The result we can figure from this is the wavelike 557.7 nm radiation variations with approximate period of 10 days increasing during SSW possible due to changing of chemical composition of mesopause region during SSW event leading to the depletion excited O2 (O(1S) precursor) at the heights below and in the mesopause.

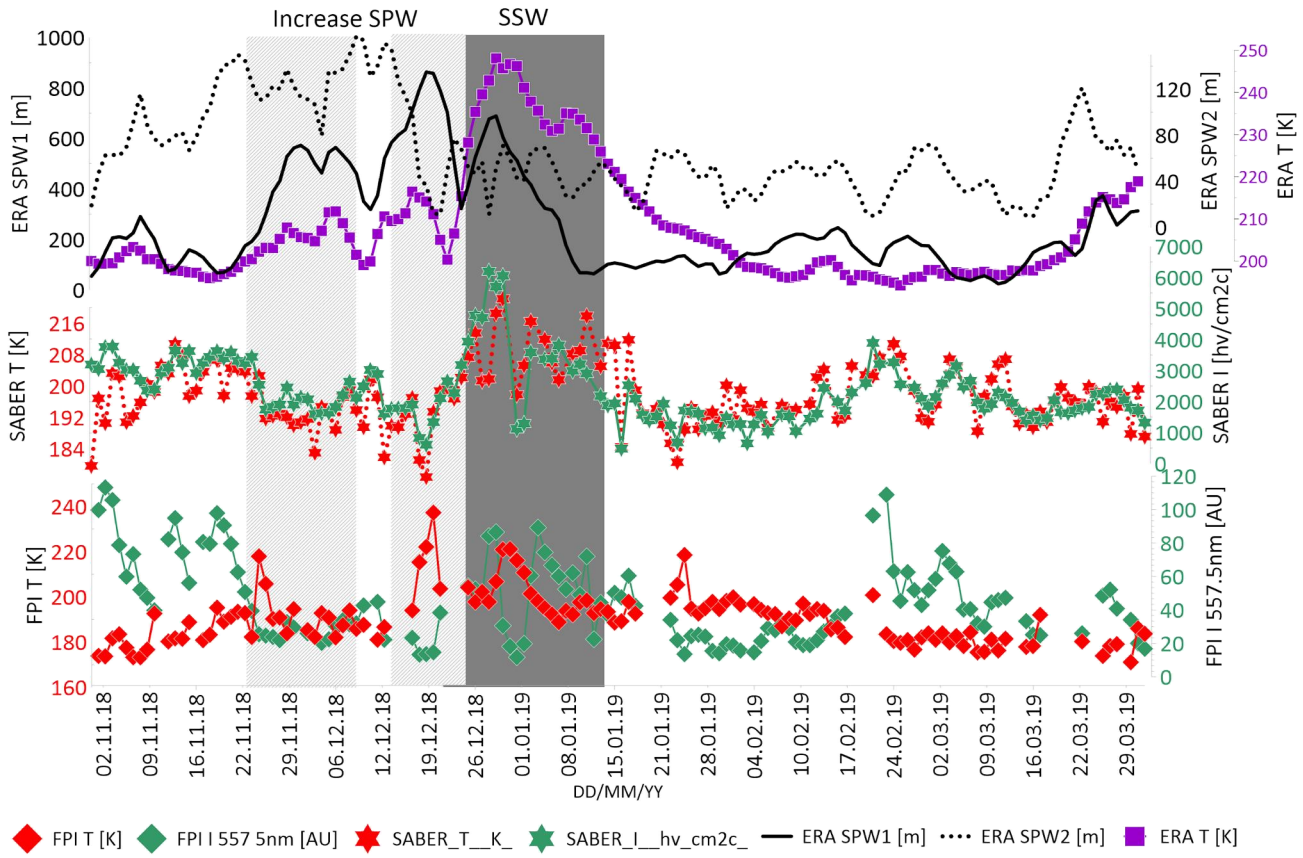

Figure 3: FPI emission 557.7 nm (green diamond), FPI temperature (red diamond), SABER temperature (red star), SABER emission 557.7 nm (green star), amplitude of SPW 1 (solid black line), amplitude of SPW 2 (dotted black line) from 01 nov 2018 to 31 Mar 2019.

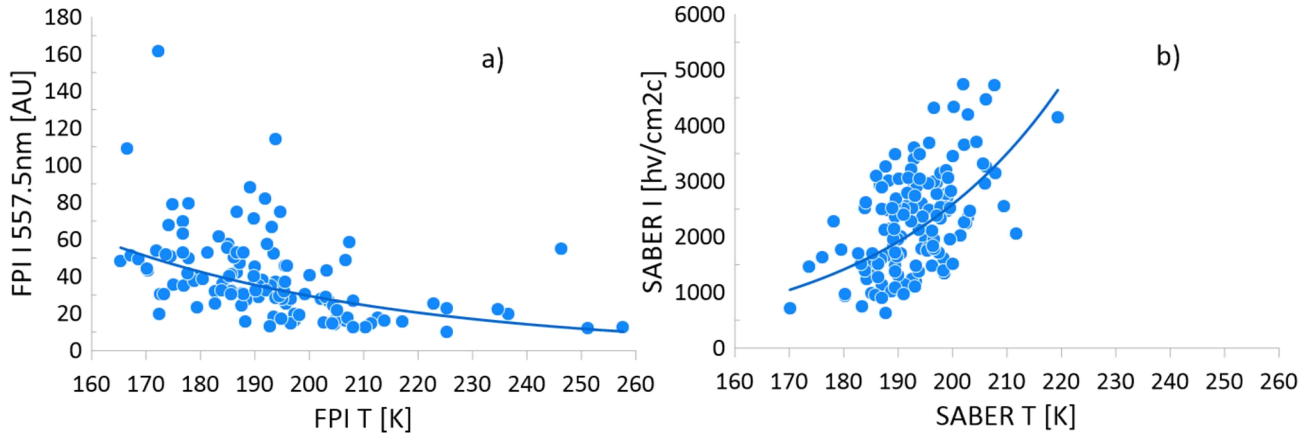

Figure 4: Dependence of temperature on emission 557.7 nm by a - FPI, b - SABER.

Our assumption about measuring the intensity of 557.7 nm at different heights according to the FPI and SABER is confirmed by the results of model calculations (Figure 5). MUAM is a new version of the COMMA-LIM model, at which the upper boundary was raised to the heights of the ionospheric layer F2 (altitude 300-400 km depending on the level of solar activity, or rather, the vertical temperature profile [18]. In recent years, new modifications of MUAM have been made: parametrization of the influence of orographic gravitational waves [19,20] has been included, parameterization has been developed and implemented normal atmospheric modes [21]. The updated version of the MUAM uses the climatological three-dimensional distribution of ozone and water vapor in the troposphere, taking into account longitudinal variations [22]. In addition, in order to take into account long-term oscillations in the tropics (El Nino South Oscillation - ENSO, Madden-Julian Oscillation - OMD), heating parametrization was implemented due to the generation of latent heat [23]. Using the latest version of the MUAM, ensemble calculations were performed for various phases of ENSO for January - March. The design of the calculated experiments was the same as in the paper [19]: the fixed zenith angle of the Sun, corresponding to January 1 and / or March 1, was set for the first 330 model days, and then seasonal changes were included. Thus, 330–400 model days correspond to the conditions of January, February, and March.

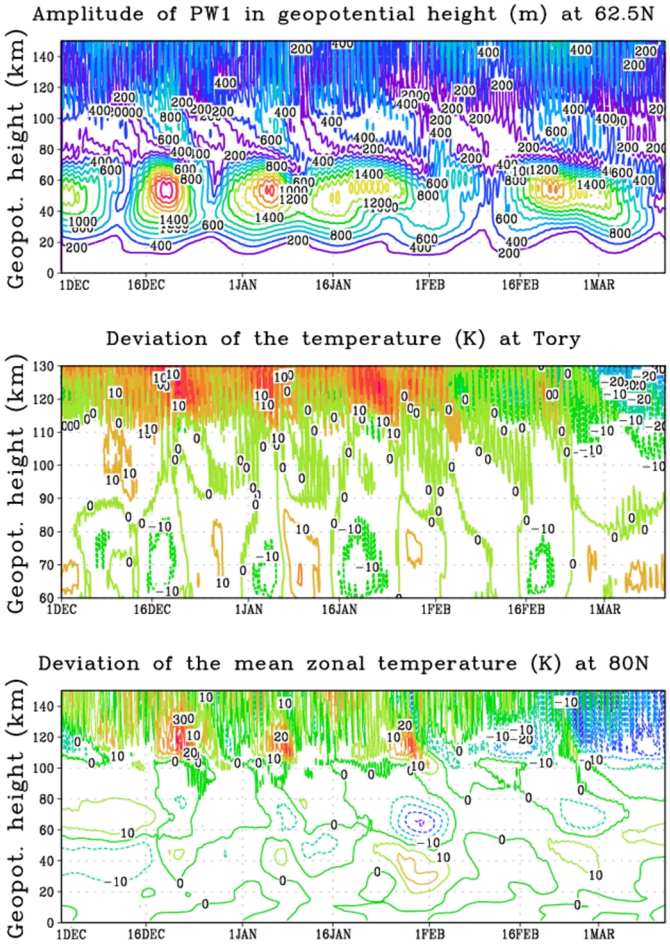

Figure 5: Top down: amplitude of SPW1 at 62.5N, deviation of temperature at Tory, deviation of mean zonal temperature at 80N by MUAM data.

We chose the most similar model run for circulation in the stratosphere of the 2018-2019 winter. We chose the most similar model run for circulation in the stratosphere of the 2018-2019 winter. As in 2018-2019, there are two periods of increase in planetary waves that preceded major stratospheric warming. Model data show that in the vertical distribution of deviation of temperature there is a boundary at an altitude of about 110 km. During the increase of SPW1 and SSW, we see an increase in temperature above 110 km and a decrease in temperature below 110 km. Moreover, this effect is observed in the average zonal temperature and in the local temperature above the Tory. And the effect is equivalent with an increase in planetary waves and with stratospheric warmings. Most likely, the differences in the SABER and FPI temperatures with decreasing airglow are associated with the registration of temperature at different heights. Based on the model data, we can assume that SABER detects temperatures below 110 km during limb measurements, where the temperature actually decreases during SPW1 and SSW. And the FPI detects altitudes above 110 km, where temperatures rise with an excited stratosphere.

4. SUMMARY

We have good agreement in the behavior of the observed VER of green oxygen line by FPI and calculated VER using the SABER products observed in the same place where FPI installed both of them dim when the planetary waves penetrate up in the mesosphere. But observed behavior of temperatures - decreasing by the SABER data and increasing by the FPI data during planetary wave enhancement is embarrassing. It is does not mean wrong operation of the any of both devices. Apparently we encountered with the problem of partial lack observation data at the heights 90-110 km and upper by the satellite. If we imagine that there is extension of the green oxygen emission layer above the mentioned altitudes range we can suppose that some part of light produced at the heights with higher temperatures. At the sufficient dimming of the green emission at the regular layer height (95-97 km) the part of light over that heights shows increasing of the temperature what is observed by FPI and modeled by MUAM. The SABER data contain no information about that heights and we calculating of the temperature at the regular layer height (95-97 km) where the temperature goes down accordingly with the model data. That's why we have disagreement in the temperature observed by the different methods.

This work was supported by the Russian Science Foundation, project No. 19-77-00009. The measurements were carried out on the instrument of Center for Common Use «Angara» [http://ckp-rf.ru/ckp/ 3056]. The authors gratefully acknowledge the access to the ECMWF ERA-Interim.

5. REFERENCES

[1] Yu, Y., Wan, W., Ning, B., Liu, L., Wang, Z., Hu, L., and Ren, Z. "Tidal wind mapping from observations of a meteor radar chain 15" Journal of Geophysical Research: Space Physics, 118, 2321–2332, https://doi.org/10.1029/2012JA017976 (2011)

[2] Wilhelm, S., Stober, G., and Brown, P.: "Climatologies and long-term changes in mesospheric wind and wave measurements based on radar observations at high and mid latitudes ", Annales Geophysicae, 37, 851–875, https://doi.org/10.5194/angeo-37-851-2019, (2019)

[3] Wilhelm, S., Stober, G., and Chau, J. L.: "A comparison of 11-year mesospheric and lower thermospheric winds determined by meteor and MF radar at 69◦ N ", Annales Geophysicae, 35, 893–906, https://doi.org/10.5194/angeo-35-893-2017, (2017)

[4] Pokhotelov, D., Becker, E., Stober, G., and Chau, J. L.: "Seasonal variability of atmospheric tides in the mesosphere and lower thermosphere: meteor radar data and simulations ", Annales Geophysicae, 36, 825–830, https://doi.org/10.5194/angeo-36-825-2018 (2018)

[5] Korotyshkin, D., Merzlyakov, E., Sherstyukov, O., Valiullin, F., "Mesosphere/lower thermosphere wind regime parameters using a newly installed SKiYMET meteor radar at Kazan (56N, 49E) "Advances in Space Research doi: https://doi.org/10.1016/j.asr.2018.12.032 (2019)
[6] B. C. G. Marques, C. A. Tepley, J. T. Fentzke, R. Eva, P. T. dos Santos, and S. A. Gonzalez, "Long-term changes in the thermospheric neutral winds over Arecibo: climatology based on over three decades of Fabry-Perot observations," J. Geophys. Res. Space Phys. 117, 16458 (2012).
[7] R. Vasilyev, M. Artamonov, A. Beletsky, G. Zherebtsov, I. Medvedeva, A. Mikhalev, and T. Syrenova, "Registering upper atmosphere parameters in east Siberia with Fabry-Perot interferometer Keo scientific 'Arinae'," Solar-Terrestrial Phys. 3, 61–75 (2017)
[8] Medvedeva I.V., A. I. Semenov, A. I. Pogoreltsev, A. V. Tatarnikov "Influence of sudden stratospheric warming on the mesosphere/lower thermosphere from the hydroxyl emission observations and numerical simulations " J. Atm. Sol.-Terr.Phys.Vol.187.-P.22-32 (2019)
[9] Semenov, A.I., Bakanas, V.V., Perminov, V.I., Zheleznov, YuA., Khomich, YuV. "The near infrared spectrum of the emission of the nighttime upper atmosphere of the Earth". Geomagn. Aeron. 42 (3), 390–397. (2002)
[10] Guiping Liu, Scott L. England, and Diego Janches. "Quasi Two-, Three-, and Six-Day Planetary-Scale Wave Oscillations in the Upper Atmosphere Observed by TIMED/SABER Over ~17 Years During 2002–2018" . Journal of Geophysical Research: Space Physics 124:11, 9462-9474. (2019)
[11] Vergasova, G.V., Kazimirovsky, E.S. "External impact on wind in the mesosphere / lower thermosphere / Solar-terrestrial physics", Issue 14, pp. 119–124. In Russian, (2009).
[12] Medvedeva, I., Ratovsky, K. "Effects of the 2016 February minor sudden stratospheric warming on the MLT and ionosphere over Eastern Siberia". J. Atmos. Sol. Terr. Phys. https://doi.org/10.1016/j.jastp.2017.09.007. (2017)
[13] Medvedeva, I.V., Semenov, A.I., Perminov, V.I., Beletsky, A.B., Tatarnikov, A.V. "Comparison of ground-based OH temperature data measured at irkutsk (52°N, 103°E) and Zvenigorod (56°N, 37°E) stations with aura MLS" v3.3. Acta Geophys. 62 (2), 340–349. https://doi.org/10.2478/s11600-013-0161-x. (2014)
[14] Vasilev R.V., Artamonov M.F., Merzlyakov E.G. "Comparative statistical analysis of neutral wind in mid-latitude mesosphere / lower thermosphere based on meteor radar and Fabry—Perot interferometer data" Solar-Terrestrial Physics. vol. 4, iss. 2. pp. 49–57. DOI: 10.12737/stp-42201808. (2018)
[15] Zorkaltseva O.S., Vasilyev R.V., Mordvinov V.I., Dombrovskaya N.S. "Dynamics of the mesosphere and lower thermosphere during sudden stratospheric warmings over the Asian region" Proceedings SPIE / 25th International Symposium on Atmospheric and Ocean Optics: Atmospheric Physics. Vol.11208. P. 112086Z. - https://doi.org/10.1117/12.2540077. (2019)
[16] M.G. Mlynczak et al. "Atomic oxygen in the mesosphere and lower thermosphere derived from SABER: Algorithm theoretical basis and measurement uncertainty". JGR Atmosphere VOL. 118, 5724–5735https://doi.org/10.1002/jgrd.50401 (2013)
[17] H. Gao, J.-B. Nee, and J. Xu, "The emission of oxygen green line and density of O atom determined by using ISUAL and SABER measurements", Ann. Geophys., 30, 695–701, doi:10.5194/angeo-30-695-2012 (2012)
[18] Pogoreltsev A.I., Vlasov A.A., Fröhlich K., Jacobi Ch. "Planetary waves in coupling the lower and upper atmosphere". J Atmos Solar-Terr Phys 69:2083–2101. https://doi.org/10.1016/j.jastp.2007.05.014 (2007)
[19] Gavrilov N.M., Koval A.V. "Parameterization of mesoscale stationary orographic wave forcing for use in numerical models of atmospheric dynamics". Izv Atm Ocean Phys 49(3):244–251. https://doi.org/10.1134/S0001433813030067 (2013)

[20] Gavrilov N.M., Koval A.V., Pogoreltsev A.I., Savenkova E.N. "Simulating influences of QBO phases and orographic gravity wave forcing on planetary waves in the middle atmosphere". Earth Planets Space 67:86. https://doi.org/10.1186/s40623-015-0259-2 (2015)
[21] Pogoreltsev A.I., Savenkova E.N., Pertsev N.N. "Sudden stratospheric warmings: the role of normal atmospheric modes". Geomag Aeron 54:357–372 (2014)
[22] Suvorova E.V., Pogoreltsev A.I. "Modeling of nonmigrating tides in the middle atmosphere". Geomag Aeron 51(1):105–115 (2011)
[23] Ermakova, T.S., Aniskina, O.G., Statnaia, I.A. et al. "Simulation of the ENSO influence on the extra-tropical middle atmosphere. Earth Planets Space" 71, 8. https://doi.org/10.1186/s40623-019-0987-9 (2019)